

**Supplementary Information for**

**Molecular interaction modes of host-defense peptide cathelicidin  
LL-37 and its mutants dictate the diverse antimicrobial activities**

Xiaofei Jin<sup>1#</sup>, Huipan Wang<sup>1#</sup>, Huayuan Tang<sup>2,3\*</sup>

<sup>1</sup> Department of Respiratory Medicine, Shenzhen Longgang Second People's Hospital, Shenzhen  
518112, P.R. China.

<sup>2</sup> Department of Engineering Mechanics, Hohai University, Nanjing 211100, P.R. China

<sup>3</sup> State Key Laboratory of Structural Analysis, Optimization and CAE Software for Industrial  
Equipment, Dalian University of Technology, Dalian 116024, P.R. China

<sup>#</sup>These authors contributed equally.

\*Corresponding Author. Email: Huayuan Tang, [htang@hhu.edu.cn](mailto:htang@hhu.edu.cn)

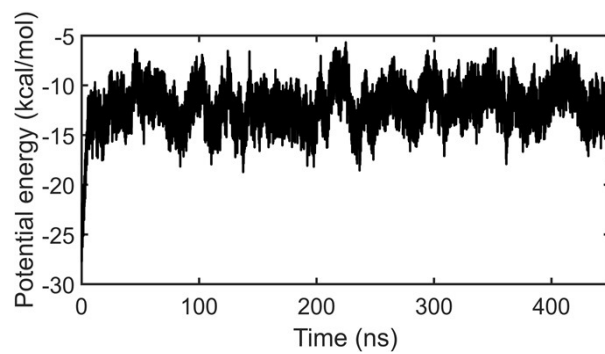


**Figure S1. Potential energy of the monomeric LL37(17-29) peptide as a function of simulation time.**

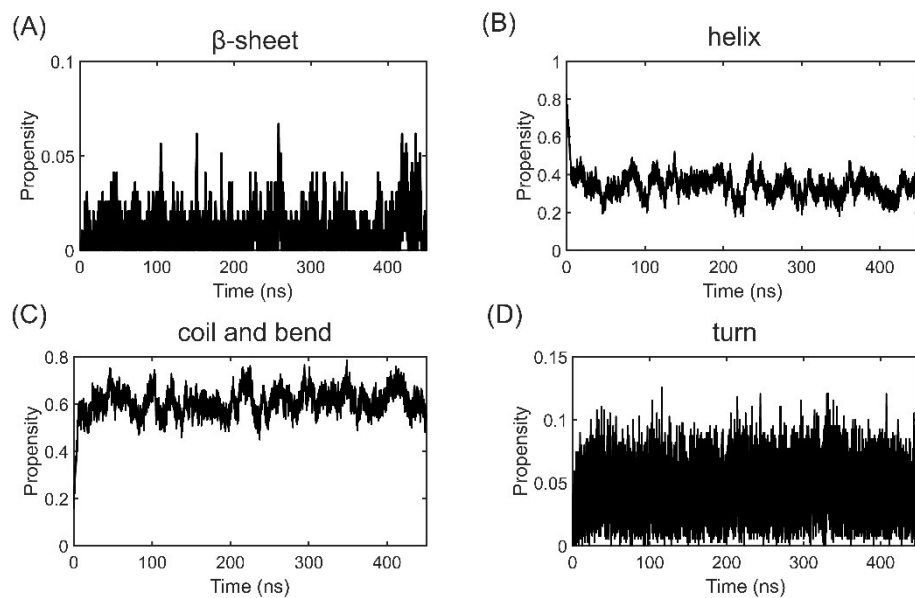


**Figure S2. Time-evolution of the secondary structure of the WT LL37(17-29) monomer. (A) Helix, (B)  $\beta$ -sheet, (C) coil and bend, and (D) turn structures.**

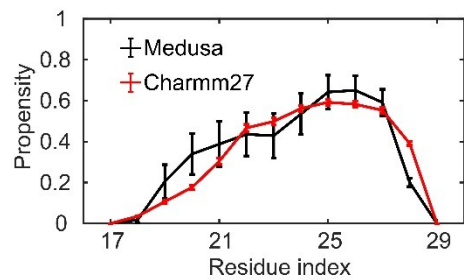


**Figure S3 Helical structure propensity of each residue of WT LL37(17-29) peptide obtained by Medusa and Charmm27 force fields.**

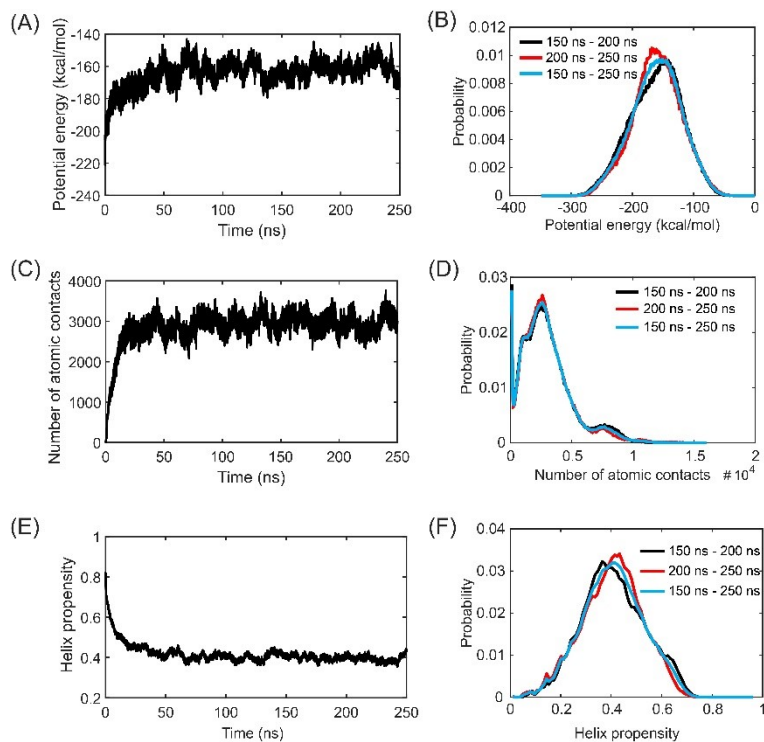


**Figure S4 Convergences of the aggregation simulations.** Evolutions of potential energy (A), the number of atomic contacts (C), and the helical property (E) of the WT LL37(17-29) peptides as a function of the simulation. Histograms of potential energy (B), the number of atomic contacts (D), and the helical property (F) during 150-200 ns, 200-250 ns, and 150-250 ns

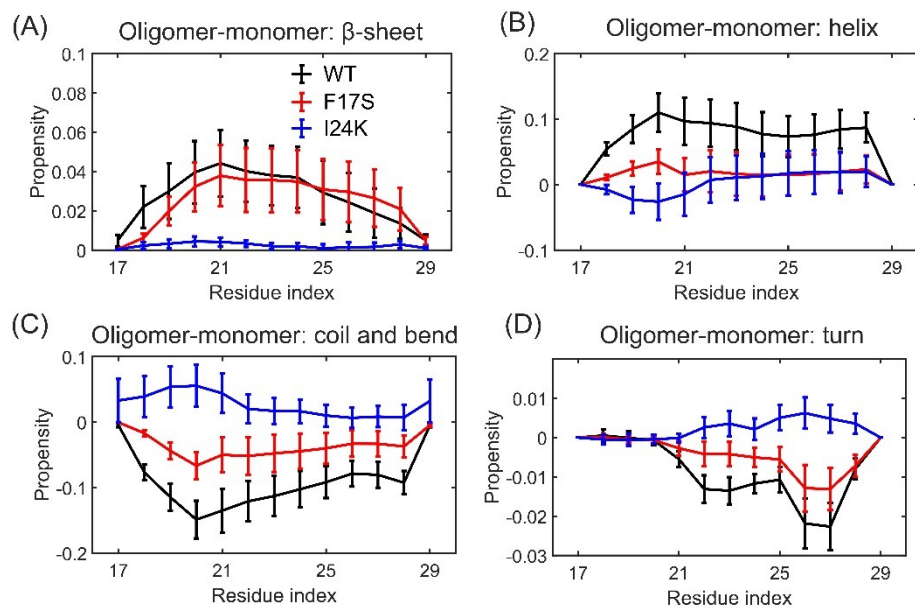


**Figure S5. Variations of the secondary structures during the aggregation of LL37(17-29) peptides and mutants. (A)  $\beta$ -sheet, (B) helix, (C) coil and bend, and (D) turn structures.**

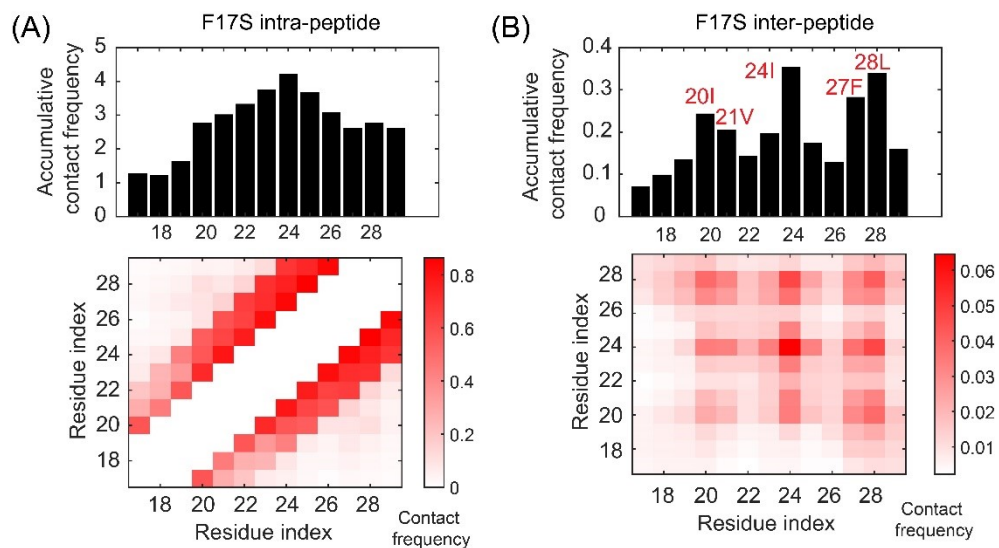


**Figure S6. Residue-wise contact frequency maps of F17S mutation.** (A) Intra-peptide contact frequency map, and (B) inter-peptide contact frequency map. The accumulative contact frequency of each residue with the rest residues are shown in the top panels.

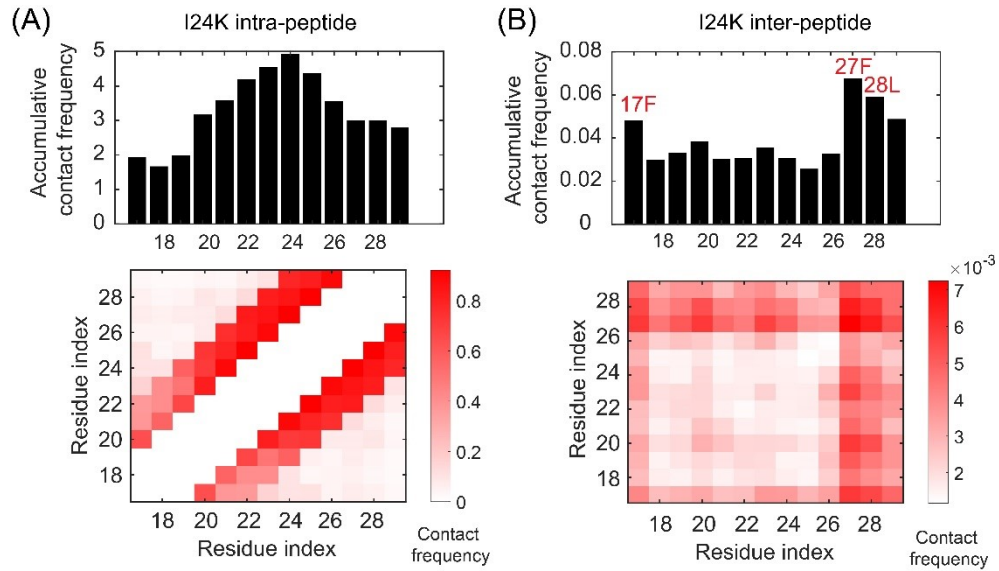


**Figure S7. Residue-wise contact frequency maps of I24K mutation.** (A) Intra-peptide contact frequency map, and (B) inter-peptide contact frequency map. The accumulative contact frequency of each residue with the rest residues are shown in the top panels.

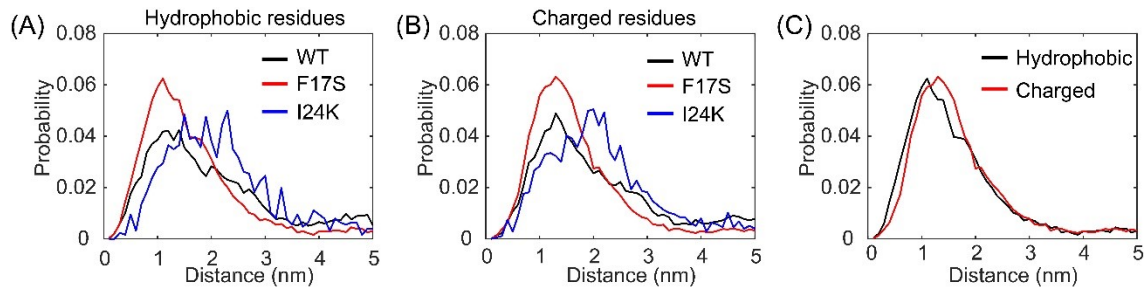


**Figure S8. Structures of oligomers formed by LL37(17-29) peptides.** Distributions of (A) hydrophobic and (B) charged residues in the oligomers formed by the WT and mutants of LL37(17-29).